Electronic Supplementary Information

Supramolecular polyelectrolyte hydrogel based on conjoined double-networks for multifunctional applications

Wen Jing Yang, Rui Zhang, Xian Guo, Ruixiang Ma, Zhiyuan Liu, Ting Wang, Lianhui Wang**

Dr. W. J. Yang, Mr. R. Zhang, Mr. X. Guo, Mr. R. Ma, Dr. T. Wang, Prof. L. Wang

Key Laboratory for Organic Electronics and Information Displays (KLOEID), Jiangsu Key Laboratory for Biosensors, Institute of Advanced Materials (IAM), Jiangsu National Synergistic Innovation Center for Advanced Materials (SICAM), Nanjing University of Posts & Telecommunications, 9 Wenyuan Road, Nanjing, 210023, China

Dr. Z. Liu

Shenzhen Institute of Advanced Technology, Chinese Academy of Sciences, 1068 Xueyuan Avenue, Shenzhen, 518055, China

E-mail: iamtingwang@njupt.edu.cn；iamlhwang@njupt.edu.cn

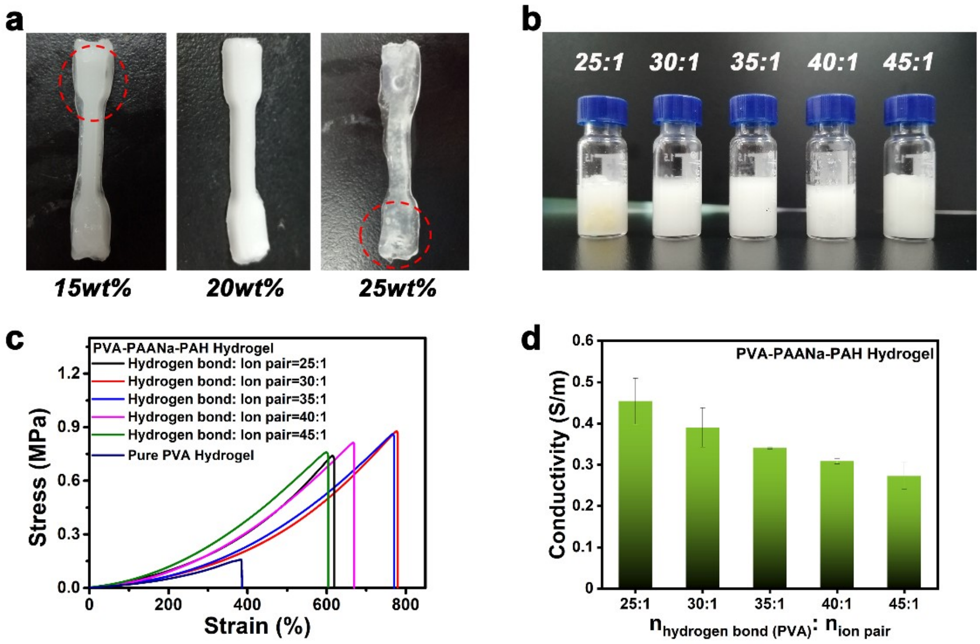

Figure S1. (a) Photos of PVA-PAANa-PAH hydrogels with different PVA contents (15 wt%, 20 wt% and 25 wt%). (b) Photos, (c) tensile stress-strain curves and (d) conductivity of PVA-PAANa-PAH hydrogels with different polyelectrolyte contents (PVA content: 20 wt%, $N_{H\text{-bonds in PVA}}$: $N_{ion\ pairs}$: 25:1, 30:1, 35:1, 40:1 and 45:1).

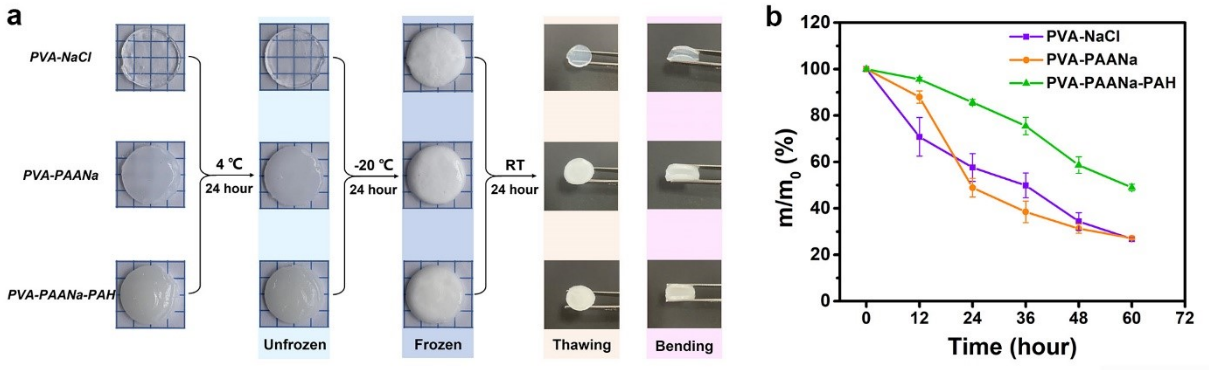

Figure S2. (a) Photos of three hydrogels after freezing and thawing process. (b) The water loss of the hydrogels at room temperature and relative humidy of 60%.

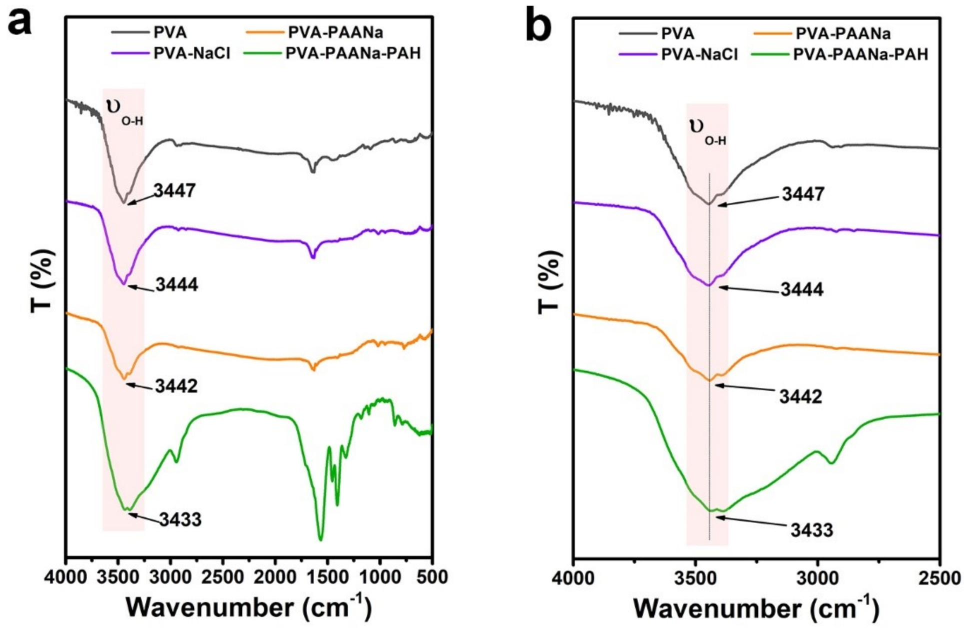

Figure S3. (a-b) FT-IR spectra of the PVA, PVA-NaCl hydrogel, PVA-PAANa hydrogel and PVA-PAANa-PAH hydrogel.

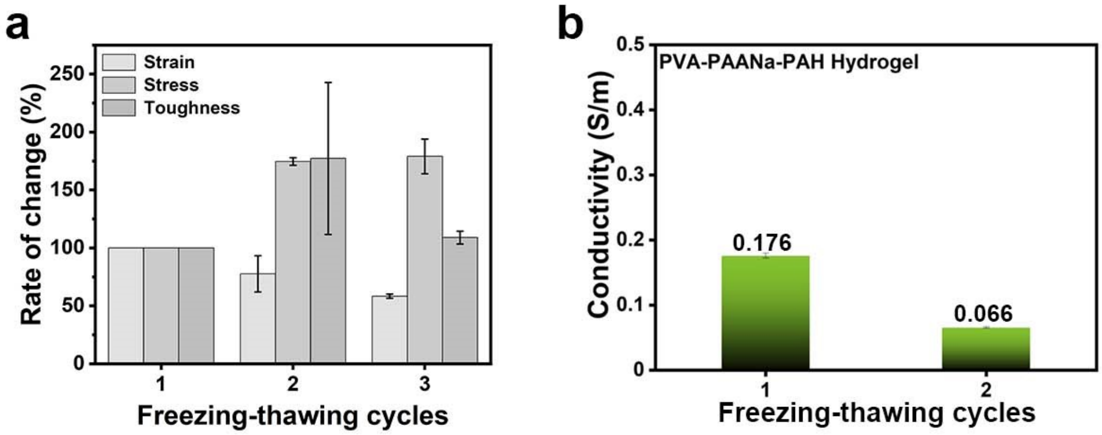

Figure S4. (a) The influences of the freezing-thawing cycles on the mechanical properties of the PVA-PAANa-PAH hydrogel. (b) The influences of the freezing-thawing cycles on the conductivities of the PVA-PAANa-PAH hydrogel.

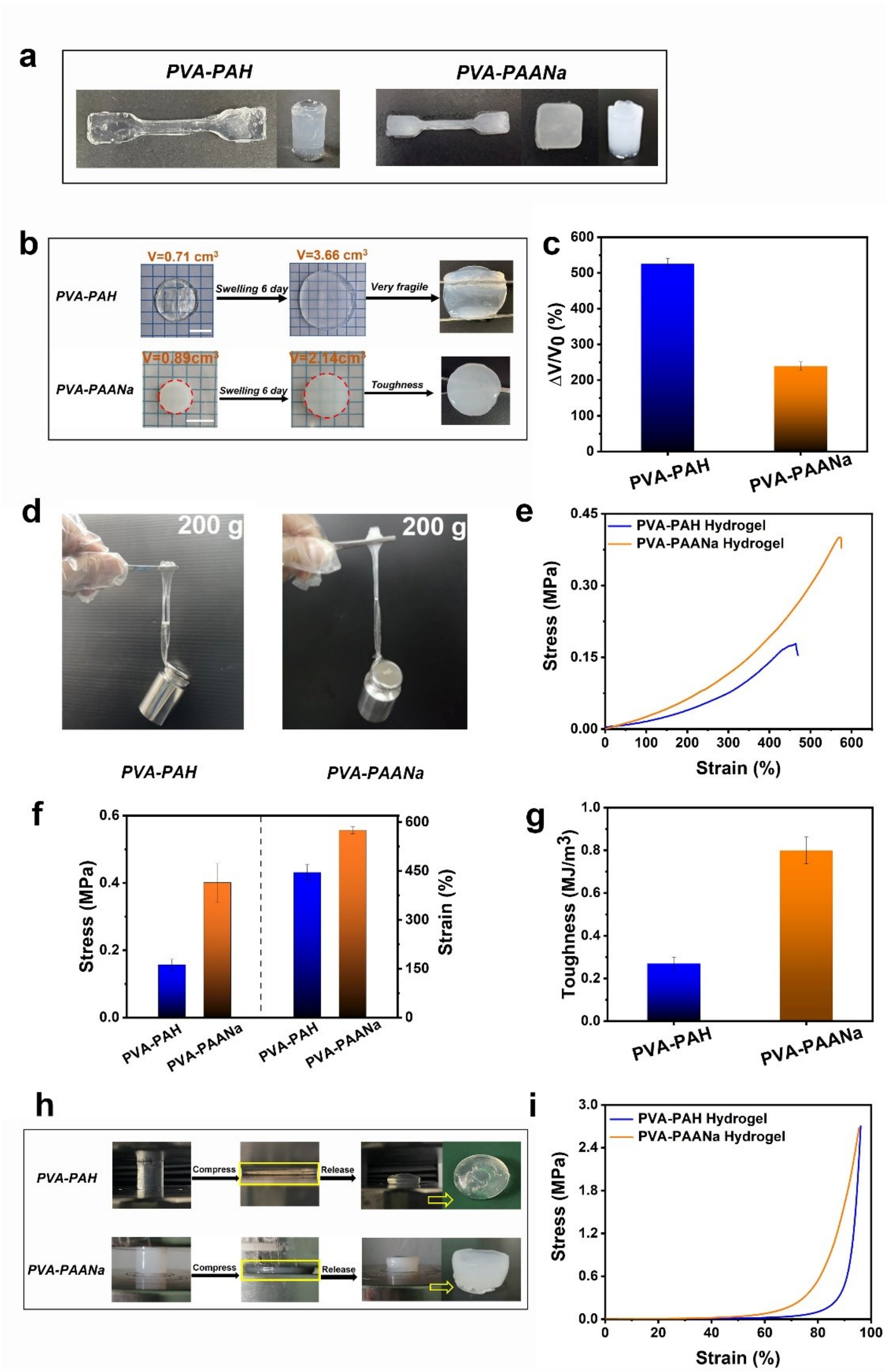

Figure S5. (a) Photos of PVA-PAH and PVA-PAANa hydrogels. (b) The swelling performances of PVA-PAH and PVA-PAANa hydrogels in water for 6 days. (c) The volume change of the hydrogels (ΔV: volume change for the hydrogels, Vo: volumne for the original hydrogels). (d) Photos of the hydrogels lifting up weight (weight of hydrogel: 0.5 g). (e) Tensile stress-strain curves, (f) the maximum stress and strain and (g) the toughness of the PVA-PAH and PVA-PAANa hydrogels. (h) Photos of the hydrogels under compression test. (i) Compressive stress-strain curves of PVA-PAH and PVA-PAANa hydrogels.

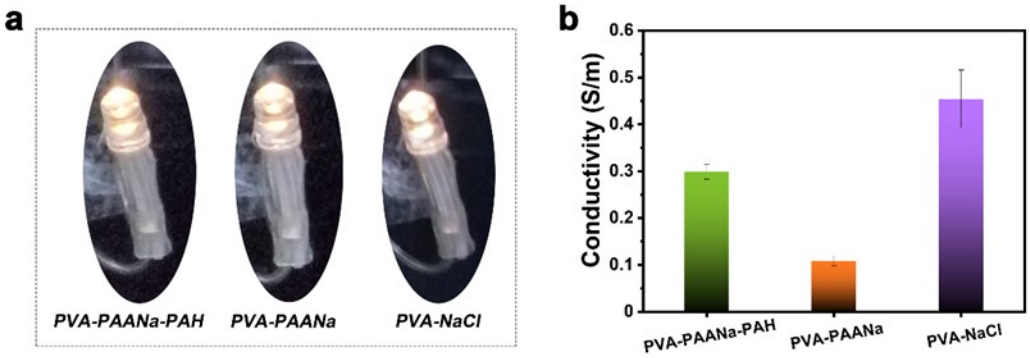

Figure S6. (a) Photos of the hydrogels as conductors to light up a LED bulb. (b) The conductivity of the hydrogels.

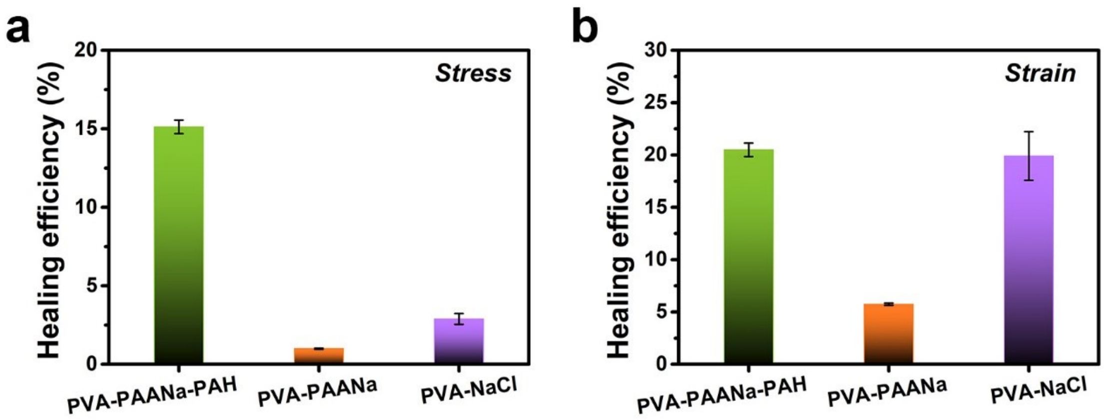

Figure S7. (a) The healing efficiencies for three hydrogels calculated by the ratio of fracture stress of original and healed hydrogels. (b) The healing efficiencies for three hydrogels calculated by the ratio of maximum strain of original and healed hydrogels.

.

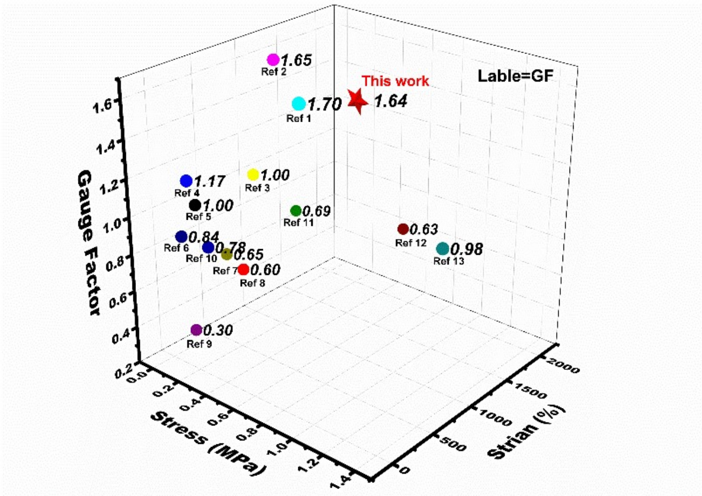

Figure S8. Comparison of gauge factor and mechanical properties with other ionic conductive hydrogels.[1-13]

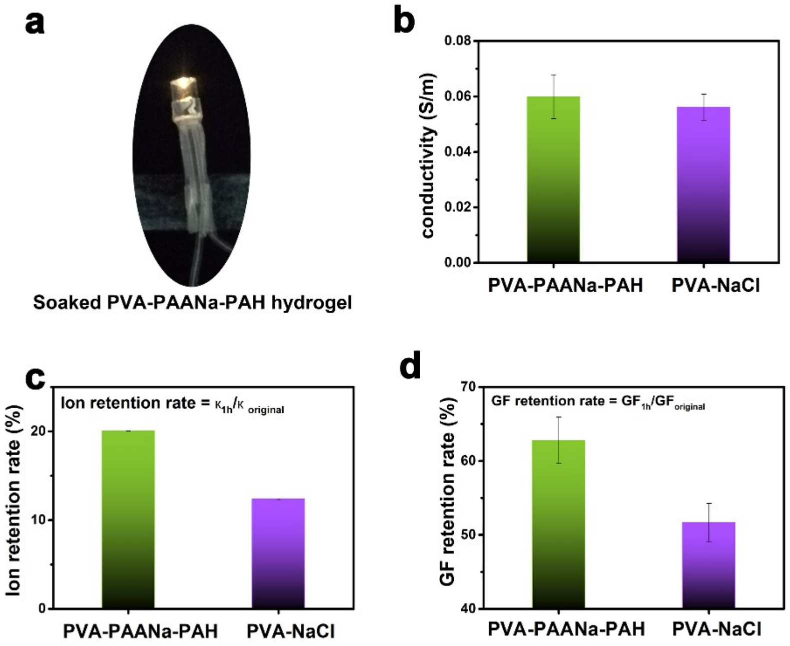

Figure S9. (a) Photo of the PVA-PAANa-PAH hydrogel as a conductor to light up a LED bulb after soaked in water. (b) The conductivity of the PVA-PAANa-PAH and PVA-NaCl hydrogels after soaked in water. (c) The ion retention rate of the PVA-PAANa-PAH and PVA-NaCl hydrogels. Ion retention rate = $\kappa_{1h}/\kappa_{original}$, where κ_{1h} and $\kappa_{original}$ are the conductivities for the hydrogels after soaked in water for 1 hour and the original hydrogels, respectively. (d) The GF retention rate of the PVA-PAANa-PAH and PVA-NaCl hydrogels. GF retention rate = $GF_{1h}/GF_{original}$, where GF_{1h} and $GF_{original}$ are the gauge factors of hydrogels soaked in water for 1 hour and the original hydrogels, respectively.

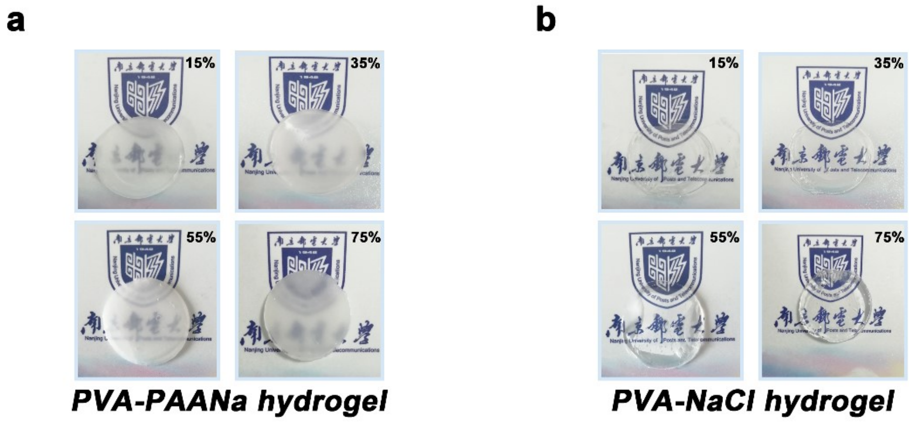

Figure S10. Photos for the hydrogels with different water content. (a) PVA-PAANa hydrogel (b) PVA-NaCl hydrogel.

References:

[1] J. Hu, Y. Wu, Q. Yang, Q. Zhou, L. Hui, Z. Liu, F. Xu, D. Ding, *Carbohydr. Polym.* **2022**, 275, 118697.

[2] H. Zheng, N. Lin, Y. He, B. Zuo, *ACS Appl. Mater. Interfaces* **2021**, 13, 40013.

[3] Z. Lei, Q. Wang, S. Sun, W. Zhu, P. Wu, *Adv. Mater.* **2017**, 29, 1700321.

[4] K. Hu, P. He, Z. Zhao, L. Huang, K. Liu, S. Lin, M. Zhang, H. Wu, L. Chen, Y. Ni, *Carbohydr. Polym.* **2021**, 264, 117995.

[5] N. Sun, F. Lu, Y. Yu, L. Su, X. Gao, L. Zheng, *ACS Appl. Mater. Interfaces* **2020**, 12, 11778.

[6] K. Tian, J. Bae, S. E. Bakarich, C. Yang, R. D. Gately, G. M. Spinks, M. I. H. Panhuis, Z. Suo, J. J. Vlassak, *Adv. Mater.* **2017**, 29, 1604827.

[7] J.-Y. Sun, C. Keplinger, G. M. Whitesides, Z. Suo, *Adv. Mater.* **2014**, 26, 7608.

[8] Y. Zhou, X. Fei, J. Tian, L. Xu, Y. Li, *J. Colloid Interface Sci.* **2022**, 606, 192.

[9] R. Tong, G. Chen, D. Pan, J. Tian, H. Qi, R. a. Li, F. Lu, M. He, *ACS Sustainable Chem. Eng.* **2019**, 7, 14256.

[10] G. Gu, H. Xu, S. Peng, L. Li, S. Chen, T. Lu, X. Guo, *Soft Rob.* **2019**, 6, 368.

[11] X. Jing, H.-Y. Mi, Y.-J. Lin, E. Enriquez, X.-F. Peng, L.-S. Turng, *ACS Appl. Mater. Interfaces* **2018**, 10, 20897.

[12] S. Liu, L. Li, *ACS Appl. Mater. Interfaces* **2017**, 9, 26429.

[13] Y. Zhou, C. Wan, Y. Yang, H. Yang, S. Wang, Z. Dai, K. Ji, H. Jiang, X. Chen, Y. Long, *Adv. Funct. Mater.* **2019**, 29, 1806220.